H. Hofbauer, C. Rathgeb, A. Uhl, and P. Wild. Iris Recognition in Image Domain: Quality-metric based Comparators. In G. Bebis et al., editors, *Proceedings of the 8th International Symposium on Visual Computing (ISVC'12)*, volume 7432 of *LNCS*, pages 1–10, Crete, Greece, July 16–18, 2012. Springer. doi: 10.1007/978-3-642-33190-9_1. The original publication is available at www.springerlink.com.

Iris Recognition in Image Domain: Quality-metric based Comparators*

Heinz Hofbauer, Christian Rathgeb, Andreas Uhl, and Peter Wild

Multimedia Signal Processing and Security Lab
Department of Computer Sciences, University of Salzburg, Austria
{hhofbaue,crathgeb,uhl,pwild}@cosy.sbg.ac.at

Abstract. Traditional iris recognition is based on computing efficiently coded representations of discriminative features of the human iris and employing Hamming Distance (HD) as fast and simple metric for biometric comparison in feature space. However, the International Organization for Standardization (ISO) specifies iris biometric data to be recorded and stored in (raw) image form (ISO/IEC FDIS 19794-6), rather than in extracted templates (e.g. iris-codes) achieving more interoperability as well as vendor neutrality. In this paper we propose the application of quality-metric based comparators operating directly on iris textures, i.e. without transformation into feature space. For this task, the Structural Similarity Index measure (SSIM), Local Edge Gradients metric (LEG), Natural Image Contour Evaluation (NICE), Edge Similarity Score (ESS) and Peak Signal to Noise ratio (PSNR) is evaluated. Obtained results on the CASIA-v3 iris database confirm the applicability of this type of iris comparison technique.

Keywords: Iris reconition, biometric comparators, image quality-metrics, image domain

1 Introduction

Iris recognition is considered one of the most reliable biometric technologies obtaining recognition rates above 99% and equal error rates of less than 1% on several data sets. Compared to other modalities, the iris offers the advantages of being extractable at-a-distance and on-the-move [12], and numerous iris feature extraction methods have been proposed continuously over the past decade [2]. Still, the processing chain of traditional iris recognition (and other biometric) systems has been left almost unchanged, following Daugman's approach [3] consisting of (1) *segmentation and preprocessing* normalizing the iris texture by unrolling into doubly-dimensionless coordinates, (2) *feature extraction* computing a binary representation of discriminative patterns of the rectified iris texture, and (3) *biometric comparison* in feature space involving the fractional HD as dissimilarity measure, see Fig. 1.

* This work has been supported by the Austrian Science Fund, project no. L554-N15 and the Austrian FIT-IT Trust in IT-Systems, project no. 819382.

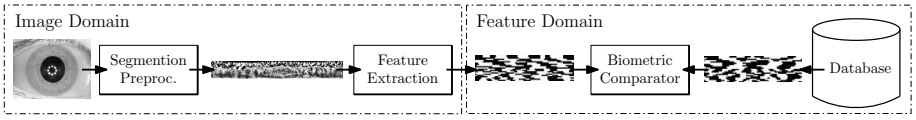

Fig. 1. Common processing chain: images are preprocessed and adaquate feature extractors generate (mostly binary) feature vectors, stored as biometric templates.

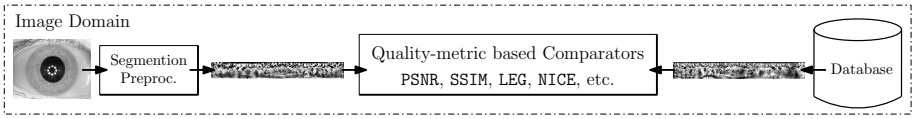

Fig. 2. Proposed processing chain: images are preprocessed and quality-metric based comparators (operating in image domain) estimate similarities between pairs of images.

In accordance with the ISO/IEC FDIS 19794-6 standard image metric-based iris biometric systems are presented. ISO/IEC FDIS 19794-6 compliant databases, which store raw iris biometric data, enable the incorporation of future improvements (e.g. in segmentation stage) without re-enrollment of registered subjects. While the extraction of rather short (a few hundred bytes) binary feature vectors provides a compact storage and rapid comparison of biometric templates, information loss is inevitable. This motivates an evaluation of comparators operating in image domain, in particular image metrics, which, to our knowledge, have not been applied to iris recognition. The contribution of this work is the application of image metrics for the purpose of iris recognition, see Fig. 2. The proposed architecture involves several benefits: (1) The problem of iris recognition can be mapped to a standard image processing problem, benefiting of results in this domain. (2) Features and comparators can be easily replaced without the necessity of re-enrollment, as the entire iris image is stored for comparison and available as reference for future comparators. (3) The approach allows for easier continuous updates, e.g. by averaging iris textures each time of successful authentication. (4) Quality-based metrics in the image domain may be combined with other image domain methods, such as SIFT-based [1] or Phase-based [9] methods. Of course, the proposed technique may also be combined with traditional feature-scale methods (in which case feature extraction has to be incorporated into the comparison module), since global features used by image metrics complement the mostly localized biometric features. (5) Finally, new techniques like [6], [14] have shown, that an incremental refinement of comparison decisions saves precious computation time and can target the drawback of traditional image quality metrics being considered slow compared to trivial metrics, such as fractional HD. Regarding the security of the stored templates it is suggested to apply standard encryption algorithms (e.g. AES) in order to protect user privacy.

The following sections are organized as follows: related work is reviewed in Section 2. The proposed approach and quality metrics are introduced in Section 3. Experiments are outlined in Section 4 using an open iris database and comparing both original as well as normalized iris images. Finally, Section 5 summarizes the paper.

2 Related Work

In the context of iris biometrics, image quality metrics are largely understood as domain-specific indicators, e.g. focus assessment or measurement of pupil/iris diameter ratio, to be considered for quality checks rejecting samples if insufficiently suited for comparison [18]. Such metrics have also been applied for dynamic matcher selection in biometric fusion scenarios [20], i.e. quality is employed to predict matching performance and to select the comparator or adjust weighting of the fusion rule. Our approach is different in employing general purpose image quality metrics and their ability to measure the degree of similarity of image pairs if one of both images is subjected to a (more or less severe) degradation in quality. In our model, the degradation of a sample to be compared is not caused by compression, but by biometric noise factors (time, illumination, etc.), and the stored biometric gallery template represents the (updated) ideal representation of the biometric property of an individual.

Pursuing the idea of employing iris comparison in the image domain, the following works need to be acknowledged: Miyazawa *et al.* [13] identify the problem of feature-based iris recognition being highly dependent on the feature extraction process varying based on environmental factors, which can be avoided by computing features in the image domain. The authors suggest to apply 2D Fourier Phase components of iris images. This scheme is extended by Krichen *et al.* [9], who propose to combine global and local Gabor (i.e. wavelet instead of Fourier coefficients) phase-correlation-based iris matching directly on enhanced (using adaptive histogram equalization) iris textures for unconstrained acquisition procedures. They employ normalized cross-correlation and a Peak to Slob Ratio (PSR) as comparator, which uses mean and standard deviation of the correlation matrix. As Local correlation-based method they correlated sub-images of fixed size using correlation peak in terms of PSR and peak position of each window computing a score out of means and standard deviation. Alonso-Fernandez *et al.* [1] propose the application of Scale Invariant Feature Transformation (SIFT) for recognition, as a means of processing without transformation to polar coordinates, thus permitting less constrained image acquisition conditions. SIFT features can be extracted from original templates in scale space and matched using texture information around the feature points. Kekre *et al.* [7], [4] use the image feature set extracted from Haar Wavelets at various levels of decomposition and from walshlet pyramid for recognition. Simple Euclidean distance on the feature set is applied as the similarity measure. Furthermore, numerous advanced iris biometric comparators have been proposed [15].

3 Iris Recognition in the Image Domain

Given an image of the human eye as shown in Fig. 3 (a), the first task is the transformation into Daugman's rubbersheet model. While any accurate segmentation technique may be applied for this task, we employ the preprocessing chain in [19]. This method applies (1) reflection removal with image inpainting, (2) assessment of edge magnitude and orientation by a Weighted Adaptive Hough

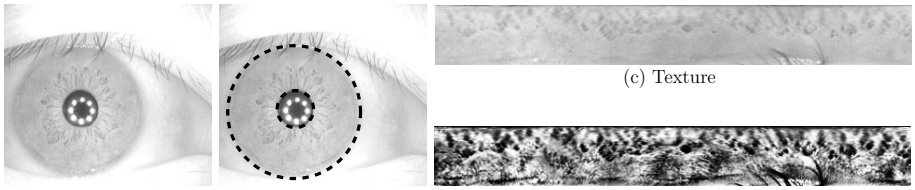

(a) Image (b) Detection (c) Texture (d) Enhanced

Fig. 3. Preprocessing: (a) image of eye (b) detection of pupil and iris (c) unrolled iris texture (d) preprocessed iris texture.

Transform for initial center detection, followed by (3) polar and ellipsopolar transforms to detect boundary candidates, which are evaluated to (4) select the most reliable ones to be used for un-wrapping the image to a rectangular texture of 512×64 pixels. Since image-based methods are largely affected by different illumination [9], we further enhance the iris texture applying CLAHE (Contrast Limited Adaptive Histogram Equalization) [22], see Fig. 3 (b)-(d).

In image-domain iris processing, we store one full reference iris texture O per user. While template-updates can easily be handled in such a scenario, for evaluations we employ enrollment using the first eye image per user only. In order to score an authentication attempt given a claimed identity, the corresponding template image O is compared with the current sample image I. Both images of $W \times H$ pixels are compared by employing one of the following quality metrics $Q(s(I,m),O)$, where $s(I,m)$ denote a shifting of m pixels to the left or right in order to obtain a rotation invariant technique. For I and O the b bits per pixel are used with a maximum pixel value of $M = 2^b$.

All of the following image metrics[1] are full reference metrics, meaning they utilize information from the original and comparison image to calculate an assessment of the visual similarity. The following subsections describe details of applied image metrics and show, which features are used in the calculation of the quality assessment.

3.1 Peak Signal to Noise Ratio (PSNR)

The PSNR is still widely used because it is unrivaled in speed and ease of use.

The following steps are performed to calculate the PSNR.

Step 1: Calculate the mean squared error $\mathrm{MSE} = \frac{1}{WH}\sum_{i=1}^{W}\sum_{j=i}^{H}(I(i,j) - O(i,j))^2$

Step 2: The PSNR is calculated:

$$\mathrm{PSNR} = 10\log_{10}\Big(\frac{M^2}{\sqrt{\mathrm{MSE}}}\Big). \tag{1}$$

[1] The implementation is available online at `http://www.wavelab.at/sources/VQI/`

3.2 Structural Similarity Index Measure (SSIM)

The structural similarity index measure (SSIM) by Wang et al. [21] uses the local luminance as well as global contrast and a structural feature to calculate a score as follows.

Step 1: Each image is transformed by convolution with a 11×11 Gaussian filter.

Step 2: The luminance, contrast and structural scores can be calculated and combined in one step as follows.

$$\mathrm{SSIM}(I,O) = \frac{(2\mu_I\mu_O + c_1)(2\sigma_{IO} + c_2)}{(\mu_I^2 + \mu_O^2 + c_1)(\sigma_I^2 + \sigma_O^2 + c_2)}, \tag{2}$$

where μ_I is the average pixel value of image I, σ_I^2 is the variance of pixel values of image I and σ_{IO} is the covariance of I and O. The variables $c_1 = (k_1 M)^2$ and $c_2 = (k_2 M)^2$, with $k_1 = 0.01$ and $k_2 = 0.03$, are used to stabilize the division.

3.3 Local Edge Gradients Metric (LEG)

The image metric based on local edge gradients was introduced by Hofbauer and Uhl [5] and uses luminance and localized edge information from different frequency domains.

Step 1: First the global luminance difference between I and O is calculated as $\mathrm{LUM}(I,O) = 1 - \sqrt{\frac{|\mu(O)-\mu(I)|}{M}}$, where $\mu(X) = \frac{1}{WH}\sum_{x=1}^{W}\sum_{y=1}^{H} X(x,y)$, and $X(x,y)$ is the pixel value of image X at position x, y.

Step 2: One step wavelet decomposition with Haar wavelets resulting in four sub images for each image X denoted as X_0 for the LL-subband, and X_1, X_2, X_3 for LH, HH and HL subbands, respectively.

Step 3: A local edge map is calculated for each position x, y in the image, reflecting the change in coarse structure of the image.

$$\mathrm{LE}(I,O,x,y) = \begin{cases} 1 & \text{if } \mathrm{EDC}(I,O,x,y) = 8, \\ 0.5 & \text{if } \mathrm{EDC}(I,O,x,y) = 7, \\ 0 & \text{otherwise.} \end{cases}$$

$$\mathrm{EDC}(I,O,x,y) = \sum_{p \in N(x,y)} \mathrm{ED}(I,O,x,y,p)$$

$$\mathrm{ED}(I,O,x,y,p) = \begin{cases} 1 & \text{if } I(x,y) < I(p) \text{ and } O(x,y) < O(p), \\ 1 & \text{if } I(x,y) > I(p) \text{ and } O(x,y) > O(p), \\ 0 & \text{otherwise.} \end{cases}$$

where $N(x,y)$ is the eight neighborhood of the pixel x, y.

Step 4: In order to assess the contrast changes a difference of gradients in a neighborhood is calculated

$$\mathrm{LED}(I,O,x,y) = \frac{1}{8}\sum_{p \in N(x,y)} \left(1 - \sqrt{\frac{|LD(I,O,x,y,p)|}{M}}\right)^2,$$

where $\mathrm{LD}(I, O, x, y, p) = (O(x, y) - O(p)) - (I(x, y) - I(p))$.

Step 5: The edge score is calculated by combining local edge conformity (LE) and local edge difference (LED) into

$$\mathrm{ES}(I, O) = \frac{4}{WH} \sum_{x=1}^{\frac{W}{2}} \sum_{y=1}^{\frac{H}{2}} \Big(\mathrm{LE}(I_0, O_0, x, y) * \frac{1}{3} \sum_{i=1}^{3} \mathrm{LED}(I_i, O_i, x, y) \Big).$$

Step 6: The LEG visual quality index is calculated by combining ES and LUM.

$$\mathrm{LEG}(I, O) = \mathrm{LUM}(I, O)\, \mathrm{ES}(I, O). \tag{3}$$

3.4 Natural Image Contour Evaluation (NICE)

The NICE quality index by Rouse and Hemami [17,16] uses gradient maps, adjusted for possible image shift by using a morphological dilation with a plus shaped structuring element. The actual score is computed by doing a thresholding on the image and calculating differences. The following steps are used to calculate the NICE score.

Step 1: Gradient amplitude image $\hat{I}$ is generated from I such that for $i \in [1, \ldots, W]$ and $j \in [1, \ldots, H]$ $\hat{I}$ is defined as $\hat{I}(i, j) = \sqrt{S_x(I, i, j)^2 + S_x(I, i, j)^2}$, where $\hat{I}(i, j)$ is the pixel value at location i, j and $S_x(I, i, j)$ and $S_y(I, i, j)$ are the results of a Sobol filter at position i, j in image I in direction x and y, respectively. Likewise $\hat{O}$ is generated from O.

Step 2: A binary image $B_{\hat{I}}$ is generated by thresholding with the average gradient amplitude value. That is, $B_{\hat{I}}(i, j) = 1$ if $\hat{I}(i, j) > T_{\hat{I}}$ and $B_{\hat{I}}(i, j) = 0$ otherwise, where $T_{\hat{I}} = \frac{1}{WH} \sum_{i=1}^{W} \sum_{j=1}^{H} \hat{I}(i, j)$.

Step 3: The binary image $B_{\hat{I}}$ is transformed into $B^+_{\hat{I}}$ by applying a morphological dilation with a plus shaped structuring element. That is, each pixel $B^+_{\hat{I}}(i, j)$ is set to 1 if at least one of the 4−connected neighbours of $B_{\hat{I}}(i, j)$ or $B_{\hat{I}}(i, j)$ is 1, otherwise $B^+_{\hat{I}}(i, j) = 0$.

Step 4: The NICE score is calculated based on the normalized Hamming distance as

$$\mathrm{NICE}(O, I) = \frac{\sum_{i=1}^{W} \sum_{j=1}^{H} (B^+_{\hat{O}}(i, j) - B^+_{\hat{I}}(i, j))^2}{\sum_{i=1}^{W} \sum_{j=1}^{H} B^+_{\hat{O}}(i, j)} \tag{4}$$

3.5 Edge Similarity Score (ESS)

The ESS was introduced by Mao and Wu [11] and uses localized edge information to compare two images.

Step 1: Each image is separate into N blocks of size 8×8.

Step 2: For each image I a Sobel edge detection filter is used on each block i to find the most prominent edge direction e^i_I and quantized into one of eight directions (each corresponding to 22.5°). Edge direction 0 is used if no edge was found in the block.

Step 3: Calculate the ESS based on the prominent edges of each block:

$$\mathrm{ESS} = \frac{\sum_{i=1}^{N} w(e_I^i, e_O^i)}{\sum_{i=1}^{N} c(e_I^i, e_O^i)}, \tag{5}$$

where $w(e_1, e_2)$ is a weighting function defined as

$$w(e_1, e_2) = \begin{cases} 0 & \text{if } e_1 = 0 \text{ or } e_2 = 0 \\ |cos(\phi(e_1) - \phi(e_2))| & \text{otherwise,} \end{cases}$$

where $\phi(e)$ is the representative edge angle for an index e, and $c(e_1, e_2)$ is an indicator function defined as $c(e_1, e_2) = 0$ if $e_1 = e_2 = 0$ and $c(e_1, e_2) = 1$ otherwise. In cases where $\sum_{i=1}^{N} c(e_I^i, e_O^i) = 0$ the ESS is set to 0.5.

4 Experiments

Experiments are carried out on the CASIA-v3-Interval iris database[2] using left-eye images only. The database consists of good quality 320×280 pixel NIR illuminated indoor images where the applied test set consists of 1307 instances, a sample is shown in Fig. 3 (a).

Recognition accuracy is evaluated in terms of false non match rate (FNMR) at a certain false match rate (FMR). The FNMR defines the proportion of verification transactions with truthful claims of identity that are incorrectly rejected, and the FMR defines the proportion of verification transactions with wrongful claims of identity that are incorrectly confirmed (ISO/IEC FDIS 19795-1), in particular, ZeroFMR defines the FNMR at a FMR of 0.1%. As score distributions overlap the Equal Error Rate (EER) of the system is defined (FNMR = FMR). At all authentication attempts 7 circular texture-shifts are performed in each direction for all comparators. A summary of obtained EERs and ZeroFMR rates at the corresponding decision thresholds for the underlying image quality metrics is given in Table 1. Receiver operating characteristics, which illustrate the tradeoff between FMR and FNMR, are plotted in Fig. 4 for experiments evaluating (a) metrics, as well as (b) impact of the used image type: original image, texture after segmentation, and enhanced texture after CLAHE normalization. Score distributions for each metric (normalized to $[0, 1]$) with respect to genuine (intra-) and impostor (inter-personal) comparisons are illustrated in Fig. 5.

4.1 Which quality metrics are useful iris biometric comparators?

With respect to accuracy, the ranking of metrics is as follows: SSIM, LEG, PSNR, NICE, and ESS, with the first three metrics exhibiting EERs of less

[2] The Center of Biometrics and Security Research, CASIA Iris Image Database, http://www.idealtest.org

Table 1. Recognition performance of Quality Metrics

Algorithm	Type	EER	ZeroFMR	Threshold
SSIM	Enhanced	3.40%	5.34%	0.868
LEG	Enhanced	3.99%	7.72%	0.785
NICE	Enhanced	5.14%	13.32%	0.526
ESS	Enhanced	9.61%	25.97%	0.311
PSNR	Enhanced	4.21%	10.33%	0.592
PSNR	Texture	18.88%	65.37%	0.478
PSNR	Image	23.01%	80.67%	0.638
Ma *et al.*	Iris-Code	1.83%	2.02%	–
Ko *et al.*	Iris-Code	4.36%	18.45%	–

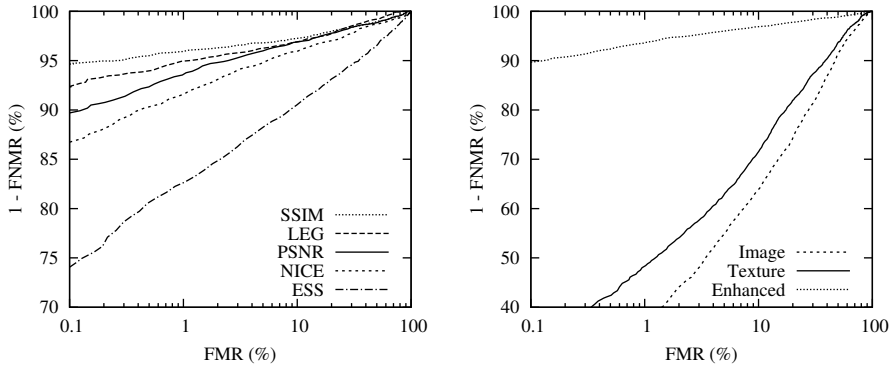

(a) Quality metrics (b) Image type (PSNR)

Fig. 4. Receiver operating characteristics by (a) quality metric, and (b) image type.

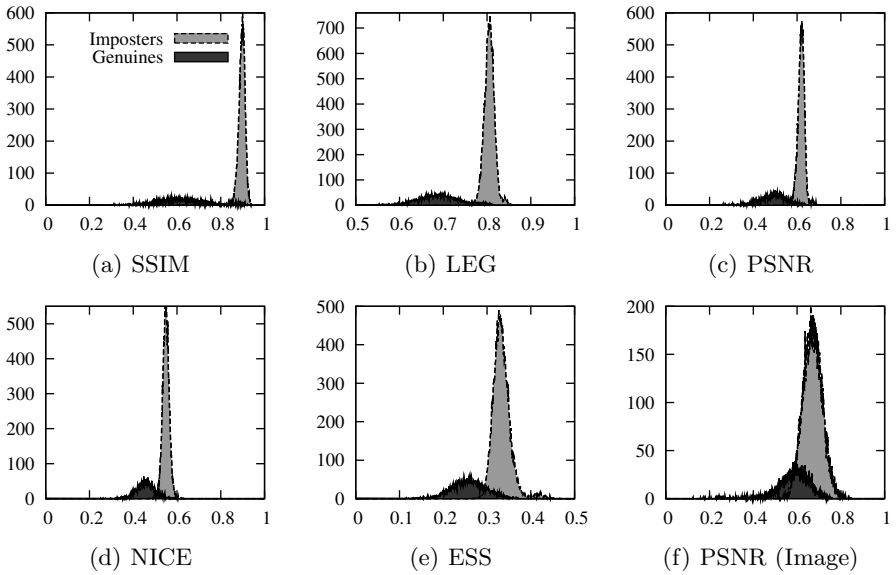

(a) SSIM (b) LEG (c) PSNR

(d) NICE (e) ESS (f) PSNR (Image)

Fig. 5. Genuine and impostor score distributions for (a) SSIM, (b) LEG, (c) PSNR, (d) NICE, (e) ESS for enhanced textures and (f) PSNR on original images.

than 5%. It is interesting to see, that PSNR with 4.21% EER performs quite well on the enhanced textures although it is the most simple metric. However, for high security applications with requested low FMR, SSIM with 5.34% ZeroFMR compared to 10.33% for PSNR is clearly the better alternative. Considering recognition accuracy image metrics do not outperform feature-based techniques [2]. For instance, on the same dataset re-implementations of the approaches of Ma *et al.* [10] and Ko *et al.* [8], which extract binary iris-codes obtain EERs of 1.83% and 4.36%, respectively (see Table 1). However, image metrics are rather useful as additional features in fusion scenarios.

4.2 How useful is texture enhancement and preprocessing?

In a second experiment, we tested the effect of texture enhancement and segmentation on iris recognition accuracy of quality metrics using PSNR as reference metric. Obtained results indicate a high degradation in case texture enhancement steps are skipped (18.88% EER instead of 4.21%). Recognition from the original eye images (without segmentation) further degraded results (23.01% EER), thus normalizaton and enhancement steps accounting for different illumination enriching the texture in the image (see Fig. 3) are extremely useful.

5 Summary

This paper applies quality metrics in image domain to the problem of iris recogniton. As opposed to the view that original iris textures exhibit too much noisy information to be used directly for comparison, we found that some metrics (SSIM, LEG, PSNR) provide quite reasonable accuracy (3.4%, 3.99% and 4.21% EER, respectively). The proposed architecture alleviates continuous template updates and enables a transparent replacement of comparators without re-enrollment. Iris texture enhancement is found to be essential to the accuracy of iris recognition in the image domain. Future work is targeted at a sophisticated analysis of fusion approaches of image-domain methods and a combination with serial comparison techniques to accelerate processing time.

References

1. Alonso-Fernandez, F., Tome-Gonzalez, P., Ruiz-Albacete, V., Ortega-Garcia, J.: Iris recognition based on sift features. In: Int'l Conf. on Biometrics, Ident. and Sec. (BIdS). pp. 1–8 (2009)
2. Bowyer, K.W., Hollingsworth, K., Flynn, P.J.: Image understanding for iris biometrics: A survey. Comp. Vis. Image Underst. 110(2), 281 – 307 (2008)
3. Daugman, J.: How iris recognition works. IEEE Trans. Circ. and Syst. for Video Techn. 14(1), 21–30 (2004)
4. H.B.Kekre, Thepade, S.D., Jain, J., Agrawal, N.: Iris recognition using texture features extracted from haarlet pyramid. Int'l J. of Comp. App. 11(12), 1–5 (2010), found. Comp. Sc.

5. Hofbauer, H., Uhl, A.: An effective and efficient visual quality index based on local edge gradients. In: IEEE 3rd Europ. Workshop on Visual Inf. Proc. p. 6pp. (2011)
6. Hollingsworth, K.P., Bowyer, K.W., Flynn, P.J.: The best bits in an iris code. IEEE Trans. on Pattern Anal. and Mach. Intell. 31(6), 964–973 (2009)
7. Kekre, H.B., Thepade, S.D., Jain, J., Agrawal, N.: Iris recognition using texture features extracted from walshlet pyramid. In: Prof. Int'l Conf. & Workshop on Emerging Trends in Techn. (ICWET). pp. 76–81. ACM (2011)
8. Ko, J.G., Gil, Y.H., Yoo, J.H., Chung, K.I.: A novel and efficient feature extraction method for iris recognition. ETRI Journal 29(3), 399 – 401 (2007)
9. Krichen, E., Garcia-Salicetti, S., Dorizzi, B.: A new phase-correlation-based iris matching for degraded images. IEEE Trans. on Systems, Man, and Cyb., Part B 39(4), 924–934 (2009)
10. Ma, L., Tan, T., Wang, Y., Zhang, D.: Efficient iris recognition by characterizing key local variations. IEEE Trans. on Image Processing 13(6), 739–750 (2004)
11. Mao, Y., Wu, M.: Security evaluation for communication-friendly encryption of multimedia. In: IEEE Int'l Conf. on Image Proc. (ICIP) (2004)
12. Matey, J., Naroditsky, O., Hanna, K., Kolczynski, R., LoIacono, D., Mangru, S., Tinker, M., Zappia, T., Zhao, W.Y.: Iris on the move: Acquisition of images for iris recognition in less constrained environments. Proc. IEEE 94, 1936–1947 (2006)
13. Miyazawa, K., Ito, K., Aoki, T., Kobayashi, K., Nakajima, H.: An efficient iris recognition algorithm using phase-based image matching. In: IEEE Int'l Conf. on Image Proc. (ICIP). pp. 49–52 (2005)
14. Rathgeb, C., Uhl, A., Wild, P.: Incremental iris recognition: A single-algorithm serial fusion strategy to optimize time complexity. In: Proc. Int'l Conf. on Biometrics: Theory, App., and Syst. (BTAS). pp. 1–6 (2010)
15. Rathgeb, C., Uhl, A., Wild, P.: Iris-biometric comparators: Minimizing trade-offs costs between computational performance and recognition accuracy. In: Proc. Int'l Conf. on Imaging for Crime Det. and Prev. (ICDP). pp. 1–7 (2011)
16. Rouse, D., Hemami, S.S.: Natural image utility assessment using image contours. In: IEEE Int'l Conf. on Image Proc. (ICIP). pp. 2217–2220 (2009)
17. Rouse, D., Hemami, S.S.: The role of edge information to estimate the perceived utility of natural images. In: Western New York Image Proc. Workshop (WNYIP). p. 4 pp. (2009)
18. Tomeo-Reyes, I., Liu-Jimenez, J., Rubio-Polo, I., Fernandez-Saavedra, B.: Quality metrics influence on iris recognition systems performance. In: IEEE Int'l Carnahan Conf. on Security Technology (ICCST). pp. 1–7 (2011)
19. Uhl, A., Wild, P.: Weighted adaptive hough and ellipsopolar transforms for real-time iris segmentation. In: Proc. Int'l Conf. on Biometrics (ICB) (2012), to appear
20. Vatsa, M., Singh, R., Noore, A., Ross, A.: On the dynamic selection of biometric fusion algorithms. IEEE Trans. on Inf. Forensics and Sec. 10(3), 470 – 479 (2010)
21. Wang, Z., Bovik, A., Sheikh, H., Simoncelli, E.: Image quality assessment: from error visibility to structural similarity. IEEE Trans. on Image Proc. 13(4), 600–612 (2004)
22. Zuiderveld, K.: Contrast limited adaptive histogram equalization. In: Heckbert, P.S. (ed.) Graphics Gems IV, pp. 474–485. Morgan Kaufmann (1994)